stellarator news

Published by Fusion Energy Division, Oak Ridge National Laboratory
Building 9201-2; P.O. Box 2009; Oak Ridge, TN 37831-8071, USA

Editor: James A. Rome Issue #7 January 1990

TJ-II approved at CIEMAT

The TJ-II project to build a Flexible Heliac in Madrid, Spain, was unanimously approved at the 31st meeting of the European Consultive Committee on Fusion Programme (CCFP).

TJ-II is designed as a 1 T medium-sized stellarator with a major radius of 1.5 m. and an average plasma radius which varies between 10 and 25 cm.The "Ad Hoc" group formed by the European Fusion Program Committee reviewed the design presented to them by the CIEMAT group on September 12–14. Their final report cited the noticeable improvements realized in the design since the machine was first proposed, namely:

- The hard core (CC/CX) will be built as one piece and be placed external to the vacuum chamber.
- The modular construction of the vacuum vessel, assembled by bolted flanges, will allow a high degree of geometrical precision.
- There is independent support for every coil and chamber.
- The design is NBI compatible.

The total cost of the machine was estimated at 32,900 MECU including power supplies and the ECH system. The detailed TJ-II design has been performed by Ansaldo AA, with the participation of DePretto-Escher Wyss, Ansaldo Ricerche, and INITEC with a strong collaboration from the EURATOM/ENEA Association at Frascati. The approved schedule calls for the first plasma in the second half of 1994.

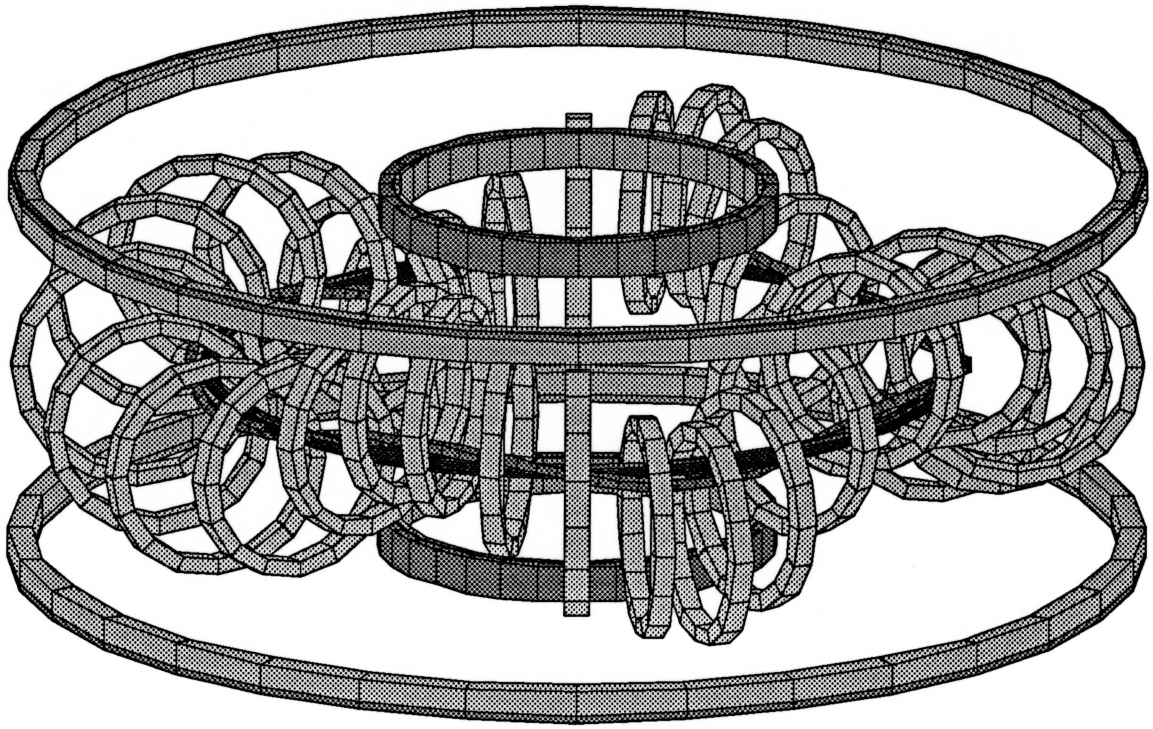

The TJ-II Flexible Heliac coil configuration

Stellarator studies at the I. V. Kurchatov IAE

Theoretical studies of the magnetic confinement of plasmas have been carried out at the I.V. Kurchatov Institute of Atomic Energy (IAE) since the very beginning of fusion research in the USSR. One of the traditional areas which has been revived in the last decade is the equilibrium and stability of plasmas in stellarators.

At the IAE, this activity is concentrated on:

- conventional stellarators (with a planar circular axis)
- Dracon systems (configurations with long straight parts and curvilinear closing elements at their ends)
- the general theory of MHD equilibrium and stability

Our studies differ from those in other fusion laboratories since they are mostly analytical.

In the theory of plasma equilibrium and stability in ordinary stellarators, the main results in the last few years were obtained within the framework of the stellarator approximation, which is based upon the ideas of Greene and Johnson. This approach was implemented to reduce the 3-D MHD equations to 2-D equations having the same structure as the analogous equations for a tokamak. Because we have been able to write the stellarator equations in forms which reduce to the familiar tokamak equations, we are able to treat both stellarators and tokamaks using a unified approach. This has allowed the direct transfer of tokamak theory methods to the solution of stellarator problems.

A short list of some problems which were investigated at the IAE includes:

- finite-β equilibria in different types of stellarators
- the analytical Mercier and ballooning criteria for stellarators
- the deformation of the rotational transform profiles in stellarators due to finite plasma pressure (generally due to a change of the configuration geometry)
- the effect of the vertical magnetic field on equilibrium configurations
- the effect of a quadrupole field on vacuum and finite-β stellarator configurations
- the effect of toroidal current on the plasma stability

Theoretical studies of the Dracon system are concentrated on the search for better CRELs (curvilinear equilibrium elements) which should not only connect the straight element ends but also stabilize the plasma. In addition, they should provide good confinement and have a comparatively simple geometry.

Vladimir D. Pustovitov
I.V. Kurchatov Institute of Atomic Energy
Moscow, USSR

Recent activities on Heliotron E: magnetic surface mapping, movable ICRF antenna, and D_2O laser system

Magnetic Surface Mapping

Magnetic surface mapping was carried out in October, as part of the optimization of the magnetic surface configuration using auxiliary toroidal and vertical field coils. For this purpose, the resistivity between the electron gun and the chamber wall is measured. The potential of the electrode with respect to the wall is 15 V, and the magnetic field strength is 4 kG (pulsed operation). The gas pressure is 3×10^{-4} Pa to prevent plasma production during the rising phase of the magnetic field. The mean free path of the residual molecules is on the order of 100 m, which means that the particles rotate 7 times around the torus. When α^* ($\equiv B_{to}/B_{ho}$) is varied, the change of the resistivity obtained experimentally agrees rather well with the calculated change of the outermost magnetic surface position.

The resistivity just inside the outermost magnetic surface has a fine structure; that is, there are several sub peaks of the resistivity within a width of 7–8 cm. This may be due to the ergodicity of the magnetic surface in the region of $\iota \geq 2$. When an error magnetic field of m/n = 1/1 mode was added, an island width of about 10 cm around the $\iota = 1$ surface was observed as expected from the calculation of the island width.

Movable ICRF Antenna

The experiment on the movable ICRF antenna started in November 1989. The antenna used is a pair of loops, each of which is fed from the same coaxial line. This antenna is inserted from the horizontal port of Heliotron E through the gate valve. It is positioned on the low-

field side. The current in each loop runs in the opposite direction from the feed point.

The objectives of this experiment are the optimization of the antenna position and angle with respect to the magnetic field and the study of the heating efficiency. The distance between the antenna and the plasma, the opening angle of the two loops, and the rotation angle around the axis of the feeder coaxial line are adjustable. The plasma loading resistance and the heating efficiency are measured by changing both the antenna and the plasma positions (inner/outer shift), and the minority ratio, field strength, and impurity amount. The antenna parameters are as follows: The feedthrough radius is 69.1 mm, and the antenna loop size is 234 × 70 mm^2. A double Faraday shield is used. The range of motion of the antenna is: horizontal shift of 650 mm, rotation angle of 360 degrees, and opening angle from 0 to 180 degrees.

Far-Infrared Thomson Scattering System for Ion Temperature Measurement

The new system for measuring ion temperature by collective far-infrared laser scattering was installed in December on the Heliotron E device. The measurement system consists of a D_2O laser (385 μm), a CW reference CD_3Cl laser (383 μm), beam transmission optics for both incident and scattered light, and a dual homodyne detection system.

Compared with conventional systems that use a heterodyne method for signal detection, improvements of signal-to-noise ratio (S/N) and frequency resolution are expected in this system, because the dual homodyne method causes no deterioration of the S/N below a certain level of stray light in the incident beam. The S/N of the dual homodyne method is the same as that of the so-called postdetection method. The scattered powers were evaluated for various plasma conditions in Heliotron E. It was shown that 200-kW output power from the D_2O laser with a pulse duration longer than 1 μs is sufficient to make the T_i measurement for neutral-beam-heated plasmas with $\bar{n}_e = (2.5–10) \times 10^{13}$ cm^{-3} and $T_i = 300–1200$ eV. It was also shown that T_i could be determined with sufficient accuracy by means of the least squares fitting of the measured spectrum to theoretical one, assuming a Maxwellian velocity distribution, and provided the postdetection S/N ratio is larger than 3. For pumping the D_2O laser, an injection locking system of TEA CO_2 lasers was constructed. Up to now, a CO_2 laser output of more than 100 J in 1 μs has been obtained, and a D_2O laser output of about 60 mJ has been obtained. The optimization of lasers is continuing. The whole system has been almost completed, and the first trial of ion temperature measurement is now planned to be done in January 1990.

Shigeru Sudo
Plasma Physics Laboratory
Kyoto University
Gokasho, Uji, 611 Japan

Status of CHS experiment

The operating magnetic field B_t of the NBI heating experiment has been extended to lower field strengths, where target plasmas are produced with second harmonic resonance of 28-GHz ECH ($B_t = 0.46–0.47$ T) and 7.5-MHz ICRF ($B_t = 0.6$ T). It was reported in the previous issue of *Stellarator News* that the NBI experiment had been done at B_t of ~ 1 T and 1.5 T. NBI-heated plasmas are now being studied in the range of B_t from about 0.5 T to 1.5 T with a variety of target plasma production methods. The ECH experiment also has been extended to a higher electron temperature regime with a simultaneous operation of 28-GHz and 53-GHz gyrotrons. Plasma parameters range as follows:

NBI with port-through power of ≤ 1.1 MW
$\bar{n}_e = (1–10) \times 10^{13}$ cm^{-3}, $T_e(0) \leq 600$ eV,
$T_i(0) \leq 550$ eV

ECH with port-through power of 120 kW (28 GHz) and 150 kW (53 GHz)
$\bar{n}_e = (0.1–2.0) \times 10^{13}$ cm^{-3}, $T_e(0) \leq 1.1$ keV,
$T_i(0) \leq 120$ eV

Confinement characteristics have been studied under the above mentioned plasma parameters: the dependence of the global energy confinement time τ_E^{exp} on B_t, n_e, P_{inj} and magnetic axis position R_{axis}. The confinement time τ_E^{exp} is defined as the stored energy W_{dia} from a diamagnetic loop divided by the deposited power, which is estimated analytically in both ECH and NBI plasmas. Absorption rates for the port-through power of 80–90% and up to 80% are employed for NBI and ECH plasmas, respectively. The decay of electron temperature after the ECH power turn-off has been measured with Thomson scattering. The experimental results show that the ECH power deposition is fairly localized to the core region, which is consistent with the analytic estimate. A comparison of τ_E^{exp} with the LHD scaling shows that the scaling is pessimistic in the low- to

medium-density regime ($\bar{n}_e < 4 \times 10^{13}$ cm^{-3}) and optimistic for high densities ($\bar{n}_e > 5 \times 10^{13}$ cm^{-3}), at which the data are scattered. Radiation loss usually increases as the density increases; in some cases more than 50% of the port-through power is radiated at high densities. The stored energy is nearly proportional to B_t in the range from 0.6 T to 1.5 T, which shows a little bit stronger dependence than the scaling. Roughly speaking, the confinement time τ_E^{exp} follows the LHD scaling.

In the course of the $\bar{n}_e$ and B_t scan, a critical (maximum) electron density $\bar{n}_e$(crit) of (8–10) $\times 10^{13}$ cm^{-3} at B_t of 1.5 T and the maximum volume averaged β value of 1.4 – 1.5% at B_t of 0.46– 0.6 T were achieved. The maximum electron density is limited by oxygen impurity radiation; above this density W_{dia} begins to deteriorate. The absolute value of the critical density and its dependence on B_t are consistent with the detached plasma concept. In high-β plasmas MHD activity has been observed at the inward-shifted magnetic axis position.

At the first International Toki Conference, the following papers were presented by the CHS group: "Review of CHS Experiment" (by K. Matsuoka et al.), " Transport Study of ECH and NBI Plasmas in CHS" (by H. Yamada et al.), "Effect of Magnetic Axis Shift on CHS Plasma Characteristics" (by S. Okamura et al.), "A Study of Radiation Collapse in CHS Plasmas" (by S. Morita et al.), "Ion Temperature and Poloidal Rotation Profile Measurements in CHS" (by K. Ida et al.), "Driven Currents in Neutral Beam Heated CHS Plasma" (by O. Kaneko et al.), "Power Deposition during ECH in CHS" (by S. Kubo et al.).

Keisuke Matsuoka for CHS group
National Institute for Fusion Science
Nagoya 464-01, Japan

Recent ATF results

Recent experiments on the ATF torsatron have extended the range of plasma parameters by using improved titanium gettering, hydrogen and deuterium pellets, careful attention to gas-feed programming, and the addition of a second 53-Ghz gyrotron. This has allowed the extension of average densities to $\bar{n}_e \leq 9 \times 10^{19}$ m^{-3} and global energy confinement times of $\tau_E \leq$ 20 ms.

During neutral beam injection (NBI), the stored energy in ATF plasmas has been observed to undergo a thermal collapse after a time which is related to the cleanliness of the vacuum vessel walls. Improvements in gettering using up to six titanium getters covering as much as ~80% of the inner-wall surface in ATF, coupled with the injection of large amounts of hydrogen or deuterium fuel coincident with NBI, have allowed NBI for about 250 ms without a thermal collapse. During NBI, the stored energy is observed to first rise to a peak, then dip, and finally rise to a second peak which is as much as two times higher than the first peak. The highest confinement times are recorded at the time of the second stored energy peak. Impurity levels were fairly low, $Z_{eff} \leq$ 2.

The measured global energy confinement time in ATF, τ_E^*, is plotted in Fig. 1 against the stellarator/torsatron empirical scaling law τ_{SL}. τ_E^* is determined by dividing the measured plasma stored energy by the total energy input from neutral beams and gyrotrons; τ_{SL}(s) = 0.17 $P^{-0.58}$ (MW) $n_e^{0.69}$(10^{20} m^{-3}) $B^{0.84}$(T) a^2(m^2) $R^{0.75}$(m).

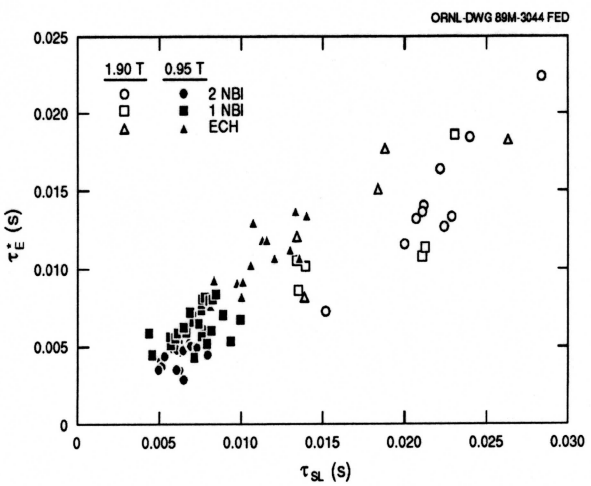

Figure 1

The positive functional dependence of τ_E^* on magnetic field is easily discerned by comparing data points at $B_0 =$ 0.95 T (solid points) and 1.9 T (open points). It should also be noted that data points exhibiting the highest confinement times are a mixture of both ECH and beam-heated discharges. NBI discharges appear in this group because the negative effect of NBI power on the confinement time is offset by the positive scaling of the density.

Figure 2 shows the maximum stored energy obtained during a large number of NBI discharges as a function of the average density. This plot contains data from one- and two-beam injected discharges at a variety of power levels. Since the stored energy is directly proportional to τ_E^*, the positive dependence of the energy confinement time on magnetic field is again in evidence upon comparing discharges with $B_0 = 0.95$ T (solid points) and 1.9 T (open points). The positive relationship between W_p^{max} (which is proportional to the confinement time) and $\bar{n}_e$ is also clearly exhibited. It may be noted that some of the highest densities shown in Fig. 2 were obtained by injecting deuterium pellets from an eight-barrel gun into a NBI discharge.

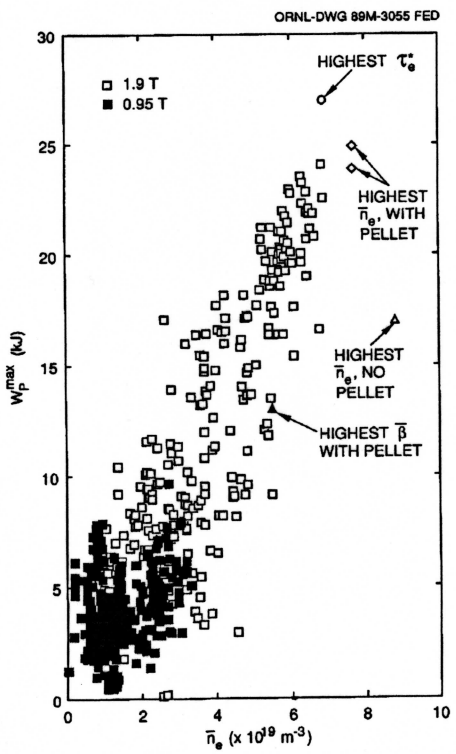

Figure 2

The optimal plasma parameters obtained in ATF (not simultaneously) are:

$\bar{n}_e \leq 9 \times 10^{13} \text{cm}^{-3}$

$\tau_E \leq 20$ ms

$W_p \leq 28$ kJ

$T_e \leq 1$ keV

$T_i \leq 400$ eV

$\beta_0 \leq 3$ %

$\bar{\beta} \leq 0.84$ %

R. J. Colchin and the ATF Group
Oak Ridge National Laboratory
P.O. Box 2009
Oak Ridge, TN 37831-8072 USA

IMS pressure cross sections

Experiments in IMS during ECR plasma production have shown that the steady-state density profiles are hollow and that a convective term in the particle balance equation is necessary to explain the profile.[1] Measurements of the plasma potential across the plasma, made on a shot-to-shot basis, indicated that the poloidal electric fields increased with the positioning of the ECR resonant layer on the outboard side of the plasma, which also increased the hollowness of the plasma profile. Based on indications that the plasma potential varied on a magnetic surface, measurements were made to examine the variation of the plasma pressure on the magnetic surfaces.

Figure 1 shows the contours of constant plasma pressure (measured using Langmuir probes) for two toroidal locations separated by 124°. Also shown in the figure are calculations of the vacuum magnetic surfaces. The relationship between the iso-pressure surfaces and the magnetic surfaces is fairly good, but the pressure on the magnetic surface can vary by up to 40%, especially in the outer regions where the density peaks.

Figure 2 shows the pressure plotted as a surface plot. The hollow pressure profile can clearly be seen throughout the plasma cross section. Significant variation in the locations of the pressure peaks is evident between the two pressure contours, which are magnetically mirror images of each other. More extensive measurements of both poloidal and toroidal variations of plasma potential are currently under way to better understand the convective terms thought responsible for these pressure variations on magnetic surfaces.

F. S. B. Anderson
Torsatron Stellarator Laboratory
University of Wisconsin
1415 Johnson Drive
Madison, WI 53706 USA

[1] J.N.Talmadge, C.A.Storlie, D.T.Anderson, F.S.B. Anderson, R.P.Doerner, P.H.Probert, J.L.Shohet and P.K.Trost, Nucl. Fusion **29** (1989) 1806.

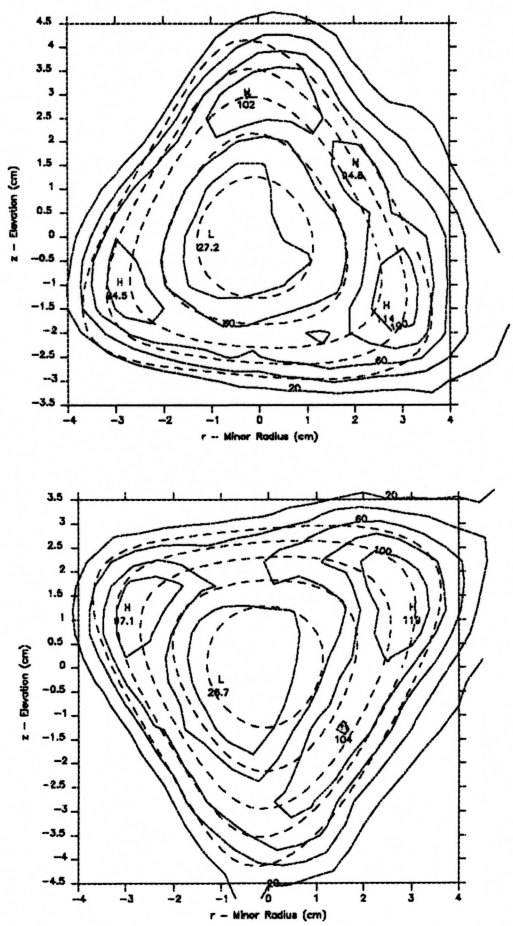

Figure 1

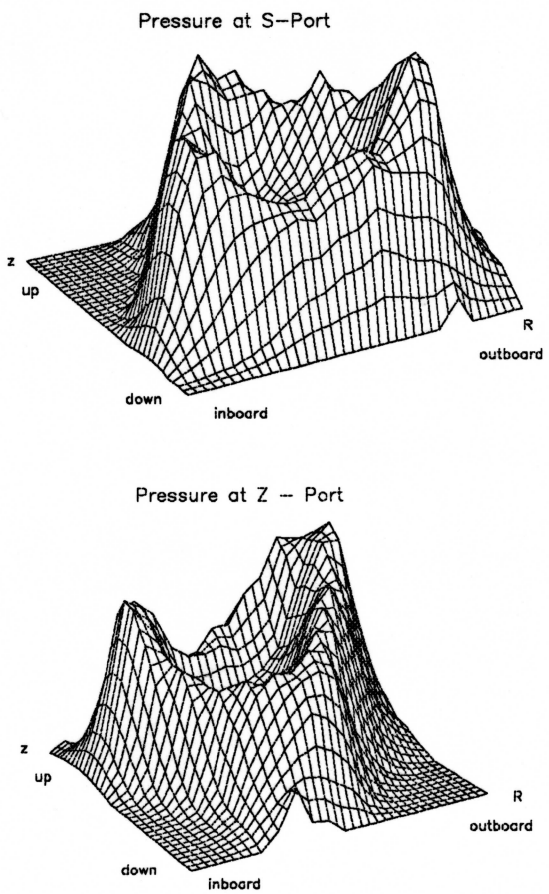

Figure 2